International Journal of Pure and Applied Mathematics
Volume 41 No. 9 2007, 1277-1288

SCIENTIFIC VISUALIZATION FOR PDES OF 2ND ORDER III: COMPARATIVE VISUALIZATION OF SOLUTIONS FOR ELLIPTIC, PARABOLIC, HYPERBOLIC AND MIXED-TYPE CASES

Lubomir Dechevsky[1 §], Joakim Gundersen[2]
[1,2]R&D Group for Mathematical Modelling
Numerical Simulation and Computer Visualization
Institute for Information, Energy and Space Technology
Narvik University College
2, Lodve Lange's St., P.O. Box 385, Narvik, N-8505, NORWAY
[1]e-mail: ltd@hin.no
[1]url: http://ansatte.hin.no/ltd/
[2]e-mail: joag@hin.no
[2]url: http://ansatte.hin.no/joag/

Abstract: This work continues the realization of the scientific visualization program outlined in [2]. Here we address the comparative visualization of the exact solutions of initial-value and boundary-value problems for parabolic, hyperbolic and elliptic PDEs of second order. For this purpose we design comparable initial and boundary conditions for the three types and use colour (mode 1) mapping (see Section 2 of [2] and the references therein) to compare the solutions as 2D colour (or grey-scale) images. The knowledge accumulated in this first part of the paper is then used in its second part for the comparative visualization of the solutions of two model mixed-type problems. One of the observable differences is the diverse behaviour of the shock waves obtained due to the propagation of singularities along the characteristic cone in the hyperbolic part of the domain of the boundary-value problem. For the visualization in the second part of the paper we use again 2D colour (mode 1) mapping, but also provide equivalent 3D modelling of the solutions as surfaces, to show the changes on the boundary between the regions of parabolicity and hyperbolicity.

Received: November 11, 2007 © 2007, Academic Publications Ltd.

§Correspondence author

Based on the graphical results, we provide some comparative analysis of the properties of the solutions in all cases. All graphical images are obtained via the in-house software developed as part of the work on [7] and [6], see also [2], [3] and [4].

AMS Subject Classification: 35A21, 35B30, 35J25, 35K05, 35K20, 35L05, 35L15, 35L20, 35M10, 65D18, 68U05, 34C30, 35B05, 35B65, 35E15, 35J15, 35K10, 35L10, 35M05, 35R05, 65D15, 65D30, 65D32, 68U20, 76M27
Key Words: comparative visualization, 3-dimensional visualization, colour map, partial differential equation, parabolic, elliptic, hyperbolic, mixed-type, initial value, boundary value, isocurve, propagation of singularities

1. Introduction

This paper is a continuation of [2] and, together with the follow-up papers [3] and [4], is dedicated to scientific visualization related to initial-value and boundary-value problems for PDEs. Our work on this topic should be considered as extension and upgrade of [6] where we discussed the scientific visualization of the numerical output of the simulator BedSim – see [6] and [2] for further details and references on BedSim.

Our purpose in this paper, as well as in [2], [3] and [4], is to show how our visualization software application discussed in [6] works on data sets generated from PDEs and their numerical approximations. We shall consider the model examples of the 3 basic types of 2nd order linear PDEs with constant real coefficients and variable right-hand side (RHS): parabolic, hyperbolic and elliptic PDE for initial and boundary-value problems on the rectangle $\{(x,t) : x \in [0,1], t \in [0,T], 0 < T < \infty\}$, that is, the space variable x will be 1D. We shall use the same model RHS for all examples of the 3 types of equations. Wherever possible, we shall use also the same model initial/boundary-value functions. Under these comparable conditions in Section 3, we shall visualize the exact (continual) solution of the boundary problem for the respective PDE.

The problem setting is as in Section 3 of [2]. In Section 2 of the present paper is given some brief orientation about this problem setting, the visualization methods and the in-house software application used in the visualization.

For the high-precision computation of fundamental solutions (Green's functions) of the parabolic, hyperbolic and elliptic problems (2), (6) and (10) in

[2] we used for the visualization in [3] low convergence-order quadrature rules (typically, the trapezium rule) with a very dense knot-vector (i.e., with small step/high resolution). This was done due to the singularities present in the graphs of the Green's functions. In the present paper we consider sufficiently smooth RHS and initial/boundary conditions, so that it is easy to obtain high convergence rates in the quadrature approximation. In this case, we use higher-order quadrature formulae, with a larger step – typically, accelerating the convergence by several iterations of Richardson extrapolation (Runge principle) via Romberg integration starting from the trapezium rule.)

After studying the basic cases of linear PDE with constant coefficients of elliptic, parabolic and hyperbolic type, we turn to a more complex problem: we consider two model examples of boundary problems for mixed-type PDEs. Based on the visualization results obtained in Section 3, we compare the propagation of the singularities (the "shock waves") of the solutions of the mixed-type using an argument founded on a celebrated theorem of Lars Hörmander ([11], Theorems 24.5.3 and 24.5.4).

2. Exact Solutions of Boundary-Value Problems for 2nd Order PDEs, Visualization Methods and Software Tools

The three scaled PDEs of parabolic, hyperbolic and elliptic type, and the respective initial-value and boundary-value problems are given in Section 3 of [2], see (2), (6) and (10) of the same section of [2], respectively. The derivation of the respective integral representation of the solutions (formulae (5), (8) and (12) in [2], respectively) is discussed in Appendices A.1, B.1 and C.1 of [2], while their approximate numerical computation is discussed in Section 3 of [2] (see also Section 1 of present paper).

Note that, unlike the case of the hyperbolic equation, in the elliptic case we do not consider the initial and boundary value problem in (6) of [2]. One reason is that in the elliptic equation the variables x and t play a symmetric role, and we thus prefer to look at (x, t) as a two-dimensional space variable, rather than a pair of a space and time variable. Another reason is that choosing initial and boundary value in (10) of [2] translates into a mixed Dirichlet - Neumann boundary value problem for the elliptic equation where Dirichlet data are given on part of the boundary, and Neumann data are given on the remaining part of this boundary. Instead, we prefer to study here the simpler Dirichlet boundary value problem as given in (10) of [2] where the data on the whole boundary are

of Dirichlet type.

The types of visualization techniques (in 3D and in variable dimensions, including higher than 3, via colour (mode 1, 2 and 3) mapping) are discussed in Section 2 of [2]. Also in this section of [2] is described our software-application used to obtain the graphical results given in this paper. This is the same software tool which was used for the visualization related to the ODE-based simulator BedSim in [6].

3. Graphical Comparison of the Solutions of the Three Basic Types for Comparable Boundary Conditions

In this section we provide comparative graphical plots based on input data sets generated from the formulae in the Section 4 of [2]. We use these graphical results to make some observations and conclusions about properties of the solutions of the three basic types of equations. The graphical plots presented are screen shots taken from the graphical output of our new software. We note that the capabilities of this software allow continuous changing of the parameters (via sliders), resulting in continuous real-time change of the form and topology of isosurfaces, isocurves, colour plots, 3D plots, etc.

In Figures 1 and 2 are shown comparative colour (mode 1) plots of the exact solutions of the three basic types of equations (2), (6) and (10) of [2] (computed with high precision using quadratures in the integral representations), for comparable boundary conditions.

Some observations and comments:

- The boundary value data and the RHS are smooth and all relevant consistency conditions are preserved.
- The initial and boundary conditions of the parabolic problem, see (2) in [2], are common also for the other two boundary-value problems (6) and (10) in [2]. To ensure comparable boundary conditions in Figures 1 and 2, the missing Neumann initial condition in (6) in [2] and Dirichlet boundary condition in (10) in [2] are recovered in two different ways described in the figures.
- Under the two sets of comparable boundary conditions, the solutions of (2), (6) and (10) of [2] vary a lot and, in particular, have fairly different range of values. Due to this, the colour scaling for the three solutions is

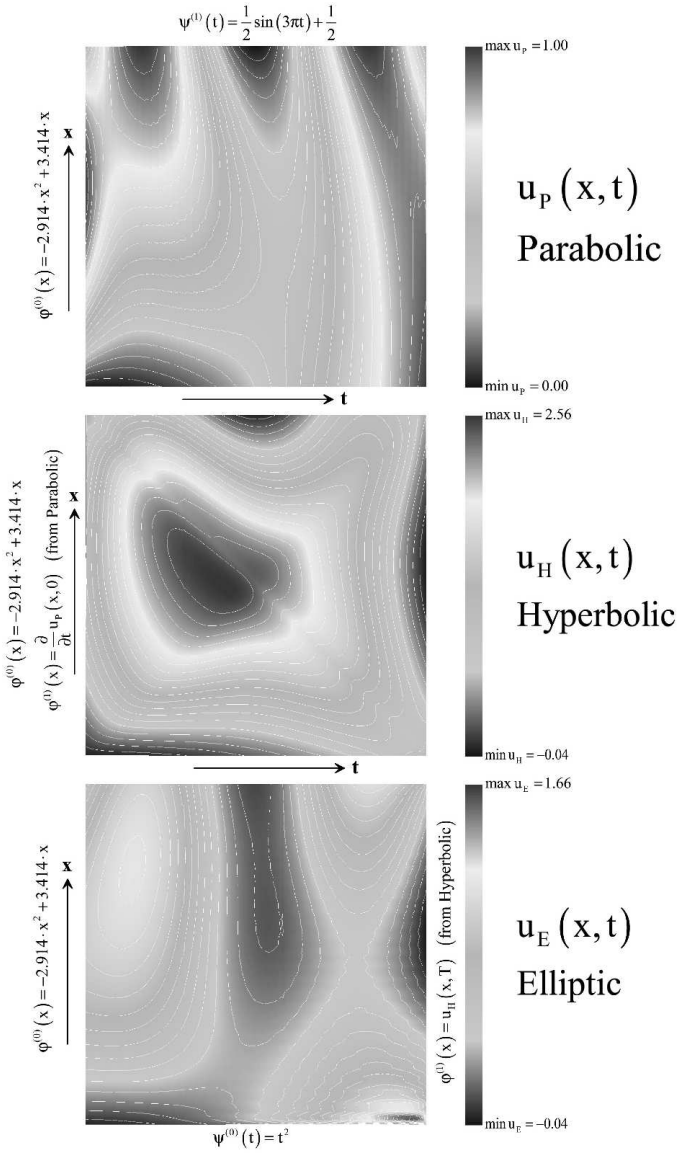

Figure 1: Comparison of the solutions for parabolic, hyperbolic and elliptic equation. The initial conditions for the hyperbolic equation are taken from the solution of the parabolic equation and the initial conditions for the elliptic case are taken from the hyperbolic solution. Here all colour maps appear as grey-scale.

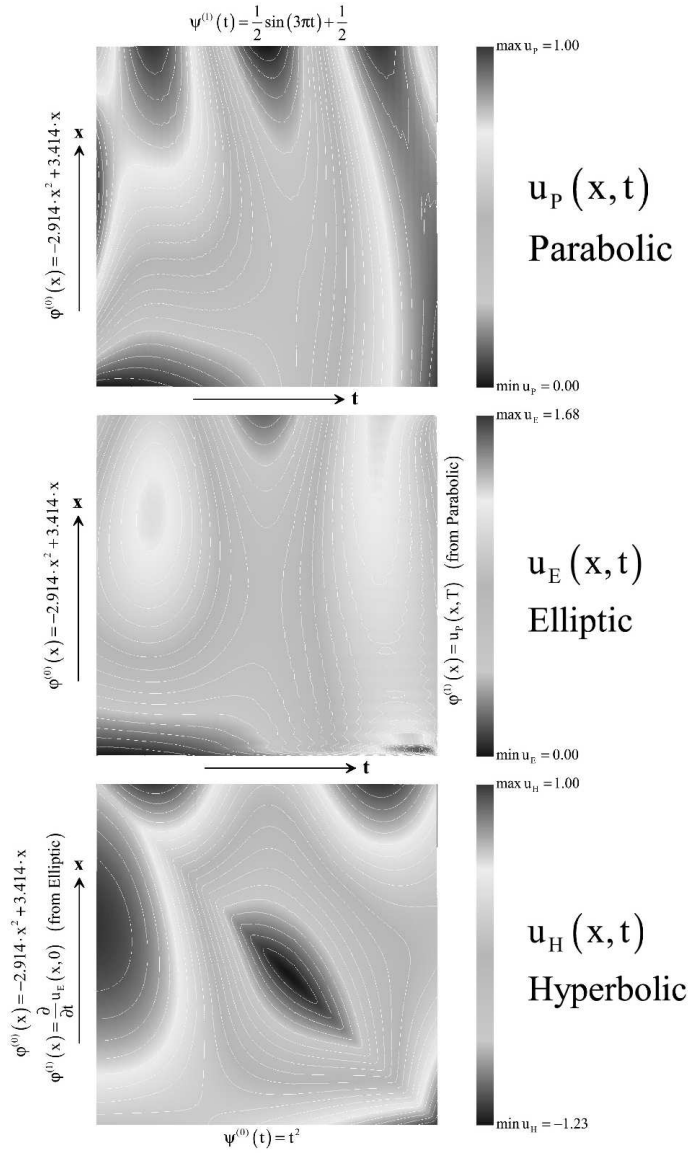

Figure 2: Comparison of the solutions for parabolic, elliptic and hyperbolic equation. The initial conditions for the elliptic equation are taken from the solution of the parabolic equation and the initial conditions for the hyperbolic case are taken from the elliptic solution. Here all colour maps appear as grey-scale.

not the same, and is described in the colour bar at the right-hand side of the respective colour plot.

- Note that in Figures 1 and 2: the solution of the parabolic problem is the same; the solution of the elliptic problem is almost the same; the solution of the hyperbolic problems varies a lot. (This has to do in part with the absence of a maximum principle in the hyperbolic case, while for the other two case there is a respective maximum principle (see, e.g., [15] and [14]).)

4. Comparative Visualization of Solutions of PDEs of Mixed Type

We are now in a position to discuss the more advanced case of visualization-based analysis of the solution of mixed-type PDEs.

We have used analytic boundary conditions and, to avoid perturbations in the exact solutions due to interference phenomena caused by interaction with the boundary, we have considered only the simple case of change of type in time in one single moment, uniformly on the whole space domain. The continuous change of type in this model would result in a very ill-conditioned numerical solution in the neighbourhood of the type change. We have avoided this by considering a discontinuous ("jump") change of type, so that the type of the equation is bounded away from degenerating, before and after the moment of change.

In Figure 3, the equation is first hyperbolic, then parabolic. The inconsistency between the boundary and the initial condition at $(x, t) = (1, 0)$ (upper left corner) causes the solution to be discontinuous there. This results in the formation of a discontinuous shock wave front along the respective characteristics in the hyperbolic region, as should be the case, according to Hörmander's theorem about propagation of the singularities along the characteristic cone, see [10], Section 24.2 and 24.5. Together with the effect of the "jump" change of type, this singular wave front is then smoothed out in the parabolic region.

In Figure 4, the sequence is reversed: first, the equation is parabolic, then, with a jump, it becomes hyperbolic. The solution is again discontinuous at $(1, 0)$, but now this is an isolated singularity, due to the smoothing effect in the parabolic region. On the contrary, the discontinuity in the moment of type change causes a shock-wave front on the hyperbolic side at this moment. If the discontinuity were isolated, then, according to Hörmander's theorem, it would

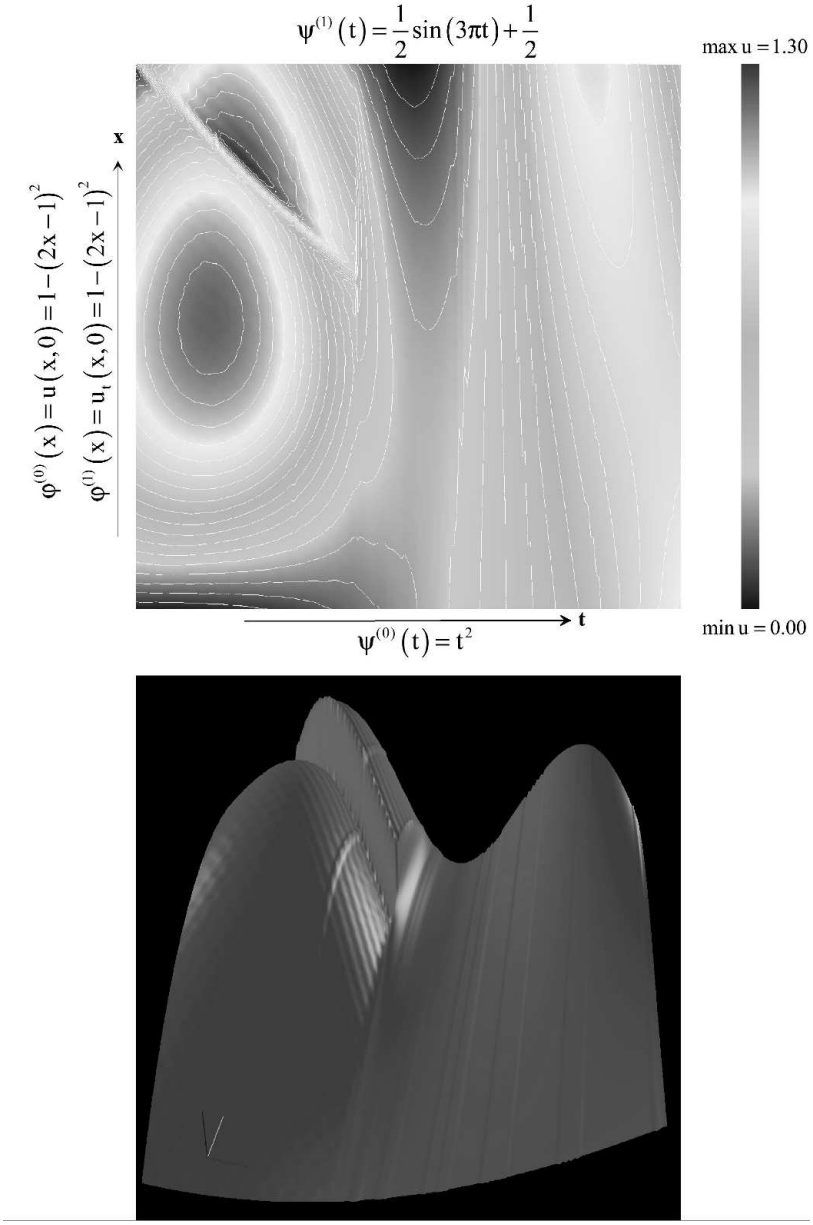

Figure 3: The solution of PDE changing from hyperbolic to parabolic equation. Here all colour maps appear as grey-scale.

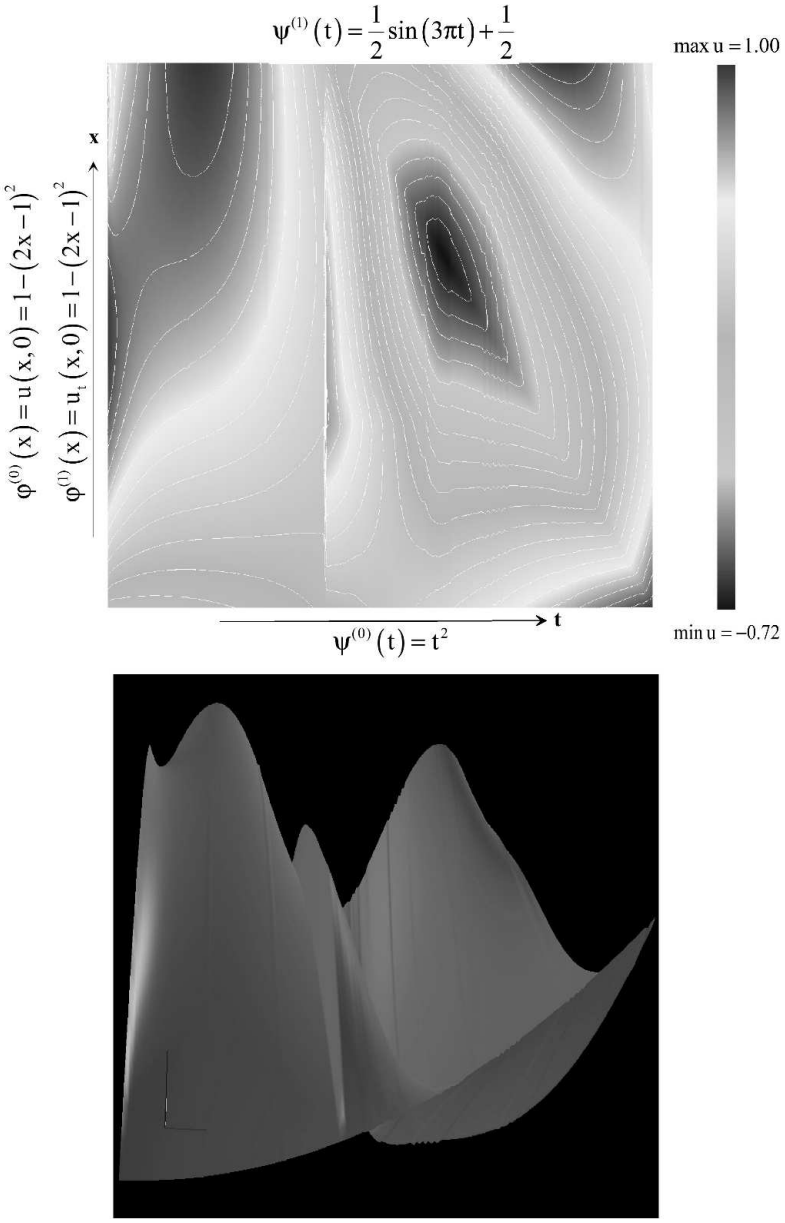

Figure 4: The solution of PDE changing from parabolic to hyperbolic equation. Here all colour maps appear as grey-scale.

have propagated in the hyperbolic region with time, but since it happens simultaneously on a whole interval in the space variable x, the resulting enveloping wave front is continuous (with modified amplitude).

These two instances of PDEs of mixed type are fairly elementary, yet they provide sufficient evidence that 3D and colour-map scientific visualization, in combination with some knowledge of the theory of PDEs and associated numerical methods, can be a basis of very useful graphical analysis and interpretation of the numerical results of the simulations in ODE-based test beds of dynamical systems even before they are upgraded with a PDE-based model. Such would be the case, in particular, with the ODE-based simulator BedSim of LKAB (see [6], [2]), the analysis of the numerical output of which was in the root of the study conducted in [2], [3], [4], and this paper.

5. Concluding Remarks

Part of the material of this paper has been announced in Section 4 of the unpublished preprint [1].

It should be noted that there are mathematically and physically meaningful boundary-value problems for strictly hyperbolic PDEs, as well as for degenerating and mixed-type PDEs with non-void hyperbolic regions, when Hörmander's theory is not valid and the singularities do not propagate along the characteristic cone. For model examples, see, e.g., the theory of the singular solutions of the so-called *Protter problem* ([12], [8], [13], [9], [5]), where the singularity remains isolated at the vertex of the characteristic cone, and does not propagate along the characteristics. Some of the references cited contain also useful scientific visualization supporting the theoretical derivations.

Of great interest is the visualization of the error distribution for iterative methods of approximate solution of non-linear ODEs and PDEs.

Acknowledgements

This work was supported in part by the 2003, 2004, 2005, 2006 and 2007 Annual Research Grants of the priority R&D Group for Mathematical Modeling, Numerical Simulation and Computer Visualization at Narvik University College, Norway.

The work of the second of the two authors was also partially supported by

a doctoral fellowship grant from LKAB, Sweden (http://lkab.com/).

References

[1] L.T. Dechevsky, J. Gundersen, From dynamical visualization of large 3D and 4D geometrical data sets to isometric conversion between dimension and resolution, *Preprint Series Narvik University College*, **3/2004**, Narvik, Norway (2004).

[2] L.T. Dechevsky, J. Gundersen, Scientific Visualization for PDEs of 2nd Order I: Problem Setting and Data Generation, *International Journal of Pure and Applied Mathematics*, **41**, No. 9 (2007), 1219-1259.

[3] L.T. Dechevsky, J. Gundersen, Scientific visualization for PDEs of 2nd order II: Comparative visualization of the Green's functions for elliptic, parabolic and hyperbolic cases, *International Journal of Pure and Applied Mathematics*, **41**, No. 9 (2007), 1261-1276.

[4] L.T. Dechevsky, J. Gundersen, Scientific visualization for PDEs of 2nd order IV: comparison between the continual and the discrete boundary value problem, *International Journal of Pure and Applied Mathematics*, **41**, No. 9 (2007), 1289-1302.

[5] L. Dechevski, N. Popivanov, T. Popov, Asymptotic expansions of singular solutions of Protter problem, *Preprint series ISSN 1504-4653, Applied Mathematics*, No. 1/2006, Narvik University College, Narvik, Norway (2006).

[6] J. Gundersen, L.T. Dechevsky, Scientific visualization for the ODE-based Simulator BedSim of LKAB, *International Journal of Pure and Applied Mathematics*, **41**, No. 9 (2007), 1197-1217.

[7] J. Gundersen, *Ph.D. Dissertation*, NTNU – the Norwegian University of Science and Technology, Trondheim, Norway, In Preparation.

[8] T.D. Hristov, N.I. Popivanov, M. Schneider, Estimates of singular solutions of Protter's problem for the 3-D hyperbolic equations, *Commun. Appl. Anal.*, **10**, No-s: 2-3 (2006), 223-251.

[9] T. Hristov, N. Popivanov, Singular solutions to Protter's problem for a class of 3-D weakly hyperbolic equations, *C.R. Acad. Bulgare Sci.*, **60**, No. 7 (2007), 719-724.

[10] L. Hörmander, *The Analysis of Linear Partial Differential Operators*, Pseudo-Differential Operators, **3**, Springer, Berlin (1985).

[11] L. Hörmander, The Analysis of Linear Partial Differential Operators. III, *Grundlehren der Mathematischen Wissenschaften [Fundamental Principles of Mathematical Sciences]*, **274**, Springer-Verlag, Berlin (1994); *Pseudo-Differential Operators*, Corrected reprint of the 1985 original.

[12] N. Popivanov, T. Popov, Estimates for the singular solutions of the 3-D Protter's problem, *Annuaire Univ. Sofia Fac. Math. Inform*, **96** (2004), 117-139.

[13] N. Popivanov, T. Popov, R. Scherer, Asymptotic expansions of singular solutions for (3+1)-D Protter problems, *J. Math. Anal. Appl.*, **331**, No. 2 (2007), 1093-1112.

[14] I. Stakgold, *Boundary Problems of Mathematical Physics*, SIAM, **2**, Philadelphia (2000).

[15] A.N. Tikhonov, A.A. Samarskii, *Equations of Mathematical Physics*, Macmillan, Pergamon Press, New York (1963).